ORAL/POSTER REFERENCE: ICF10042OR

2D SIMULATION OF TENSILE BEHAVIOR OF FIBER-REINFORCED BRITTLE MATRIX COMPOSITES WITH WEAK INTERFACE

S. Ochiai, S. Kimura, M. Tanaka and M. Hojo

Mesoscopic Materials Research Center, Graduate School of Engineering,
Kyoto University, Sakyo-ku, Kyoto 606-8501, Japan

ABSTRACT

The shear lag analysis was combined with the Monte Carlo method, and applied to two-dimensional model composite to simulate the tensile behavior of unidirectional continuous fiber-reinforced brittle matrix composites with weak interface. The features particular to weakly bonded composites such as intermittent breakage of components and interfacial debonding, serrated stress-strain curve, pull-out of fibers, deleterious effects of residual stresses on strength of composite, overall unnotched strength determined by fiber bundle, longitudinal cracking arising from the tapered portion in unnotched specimen and from the notch tip in notched specimen and the notched strength given by the net stress criterion, were simulated well.

KEYWORDS: tensile behavior, simulation, unidirectional composite, weak interface, damage map

INTRODUCTION

When the interface in brittle fiber/brittle matrix composites is strong, the crack arrest-capacity is low and high strength and toughness cannot be achieved. Thus the interface is controlled to be weak. For the design and practical use, it is needed to describe and predict the behavior of weakly bonded composites.

Under tensile load, damages (breakage of fiber and matrix, and interfacial debonding) arise at many places, being distributed spatially. The damages interact mechanically to each other. Such mechanical interactions determine the species and location of the next damage, one after another. Thus the damage map and therefore the mechanical interaction among damages vary with progressing fracture. As a result of consecutive variation of them, mechanical properties such as stress-strain curve, strength and fracture morphology are determined. Thus, for description of the behavior of composites, as the damage map varies at every occurrence of new damage, the new interaction shall be calculated for the new damage map one after another

One of the tools to solve this problem may be the shear lag analysis [1,2]. However, the ordinary shear lag analysis have been developed using the approximation that only fibers carry applied stress and the matrix acts only as a stress-transfer medium. Due to this approximation, it had two disadvantages; it can be applied only to polymer- and low yield stress-metal –matrix composites but not to intermetallic compound- and ceramic-matrix ones; and the residual stresses cannot be incorporated. Recently, the authors [3-5] have proposed a modified method to overcome

these disadvantages, with which the general situation (both fiber and matrix carry applied stress and also act as stress transfer media) can be described and residual stresses can be incorporated, to a first approximation.

In the present study, the modified shear lag analysis mentioned above will be combined with the Monte Carlo method and be applied to 2D model, to simulate the tensile behavior of unidirectional weakly bonded brittle matrix composites.

MODELING AND SIMULATION METHOD

A two-dimensional model composite employed in the present work is shown in Fig.1. The components (fiber and matrix) were numbered as 1,2,…i,... to N from left to the right side. Each component was regarded to be composed of k+1 short component elements with a length Δx. The position at x=0 was numbered as 0 and then 1, 2, 3,...j... k+1 downward, in step of Δx.. The "i" component from x=(j-1) Δx to jΔx was named as the (i,j)-component-element, and the interface from x=(j-1/2) Δx to (j+1/2) Δx between "i" and "i+1" components as the (i,j)-interface-element. The displacement of the (i,j)-component-element at x=jΔx was defined as $U_{i,j}$. Two parameters ($\alpha_{i,j}$ and $\gamma_{i,j}$) were introduced to express whether (i,j)-interface is debonded ($\alpha_{i,j}$=0) or not ($\alpha_{i,j}$=1) and whether (i,j)-component is broken ($\gamma_{i,j}$=0) or not ($\gamma_{i,j}$ =1). From the spatial distribution of debonded interface-elements with $\alpha_{i,j}$=0 and broken component-elements with $\gamma_{i,j}$=0, the damage map was expressed. The values of $\alpha_{i,j}$ and $\gamma_{i,j}$ were determined at each occurrence of damage. The values of $U_{i,j}$ were calculated by the procedure elsewhere [3,4], from which the tensile stress $\sigma_{i,j}$ of each component and shear stress $\tau_{i,j}$ at each interface were calculated .

The simulation of the stress-strain behavior was carried out in the following procedure.

(1)The strength of each component $S_{i,j}$ was determined by generating a random value based on the Monte Carlo procedure using the Weibull distribution.

(2)Two possibilities arise for the occurrence of damage; one is the fracture of the component which occurs when the exerted tensile stress $\sigma_{i,j}$ exceeds the strength $S_{i,j}$ and another is the interfacial debonding which occurs when the exerted

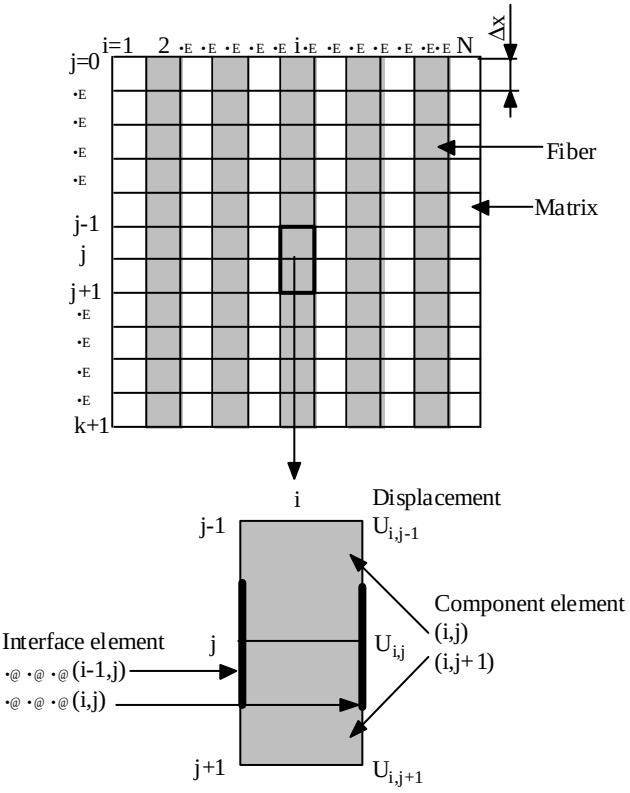

Figure1 Modeling for simulation.

shear stress $\tau_{i,j}$ exceeds the shear strength τ_c. To identify which occurs, $\sigma_{i,j}$ for all component elements were calculated and the component element having the maximum $\sigma_{i,j}/S_{i,j}$ -value, say (m,n)-component , was identified. Also, the interface element with the maximum shear stress, say (m',n'), was identified. (i)If $\sigma_{m,n}/S_{m,n}<1$ and $\tau_{m',n'}/\tau_c <1$, no breakage of component and no interfacial debonding occur. Thus the applied strain was raised. (ii)If $\sigma_{m,n}/S_{,m,n}>=1$ and $\tau_{m',n'}/\tau_c <1$, (m,n)-component-element is broken. If $\sigma_{m,n}/S_{m,n} <1$ and $\tau_{m',n'}/\tau_c>=1$, (m',n')-interface-element is debonded. If $\sigma_{m,n}/S_{m,n} >=1$ and $\tau_{m',n'}/\tau_c>=1$, (m,n)-component-element is broken when $\sigma_{m,n}/S_{,m,n}>\tau_{m',n'}/\tau_c$, while (m',n')-interface-element is debonded when $\sigma_{m,n}/S_{im,n} <\tau_{m',n'}/\tau_c$. In this way, what kind of damage occurs is identified. Then a similar process was repeated and the next damage was identified one after another. Such a procedure was repeated until no more occurrence of damage at a given strain.

(3)When no more damage occur, the applied strain ε_c was raised, and the procedure (2) was repeated until overall fracture of the composite.

RESULTS AND DISCUSSION

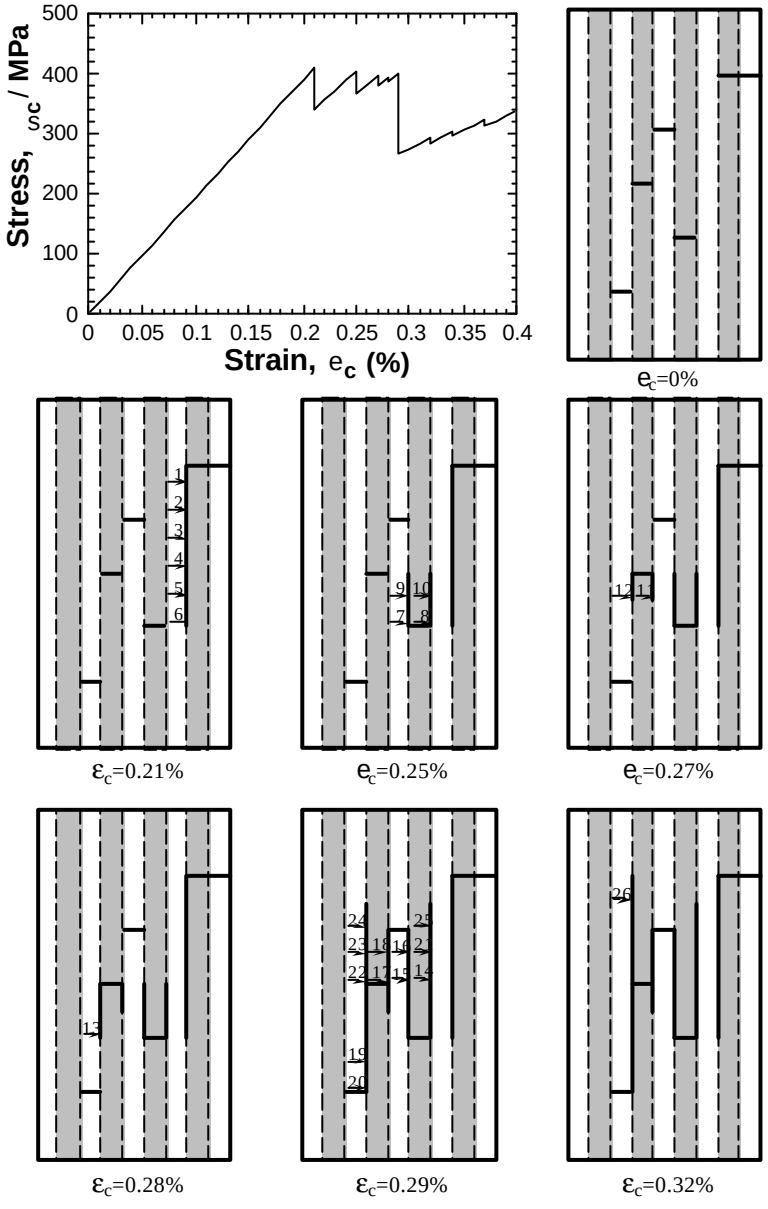

Figure 2 An example of the stress-strain curve and variation of damage map of the composite caused by progress of the interfacial debonding under the given geometry of the

broken components.

Progress of Interfacial Debonding and the Resultant Stress-strain Curve of the Composite with the Fixed Geometry of Broken Components

In this work, a mini sized model composite was used to describe the fundamental process of fracture, and following values were used for calculation: N=9, k=12, $d_f=d_m$=0.1mm, Δx= 0.2 mm (=$2d_f$), E_f=400GPa, E_m=200GPa, G_f=160 GPa, G_m=80GPa, τ_c= 50- 200 MPa. and τ_f =0 MPa.

First, in order to know the influence of pre-existent broken component element on the progress of debonding, the change of damage-map and overall stress-strain curve of composite was simulated under the given geometry of the broken components. In this case, it was assumed that no breakage of the components occurs. Figure 2 shows the stress (σ_c)-strain (ε_c) curve and damage map at various strains.

The feature of the debonding progresses is read as follows. The first debonding starts at ε_c=0.0021, followed by the 2nd to 6th debonding at the same strain, as indicated by 1 to 6. Then the debonding stops. Due to the progress of debonding at many interface-elements, the stress-carrying capacity of composite is reduced. The reduction of stress at ε_c=0.0021 in the curve corresponds to such an interfacial debonding-induced bss of stress carrying capacity. After occurrence of the 1st to 6th debonding at ε_c =0.0021, the overall debonding stops since the shear stresses of all bonded interface-elements become lower than the critical value at this strain. Beyond ε_c=0.0021, no debonding occurs and the composite stress increases up to ε_c=0.0025, at which the 7th to 10th debonding occur one after another, resulting in loss of stress carrying capacity. After the stoppage of debonding, the composite stress again increases with increasing strain. As shown in this example, the overall debonding progresses intermittently with repetition of growth and stoppage, resulting in the serrated stress-strain curve.

Stress-strain Curve of the Composite in Which Both Breakage of Components and Interfacial Debonding Occur

Figure 3 shows examples of the stress-strain curve of the composite in which both breakage of components and debonding of interface occur consecutively. (a) shows the case where the coefficients of thermal expansion of fiber(α_f) and matrix(α_m) are the same ($5x10^{-6}$/K) and therefore no residual stress exists and (b) the case where they are different(α_f =$5x10^{-6}$/K and α_m=10x 10^{-6}/K) and the residual stresses are introduced by cooling from 1500K to 300K. As the number of elements of broken fiber (N_F), matrix (N_M) and interface (N_I) were quite different to each other and could not be clearly shown on the same scale, the normalized values with respect to the final values $N_{F,f}$, $N_{M,f}$ and $N_{I,f}$, respectively, are shown in this figure. Figure 4 shows the fracture process of unnotched composite with tapered grip portion. From Figs.3 and 4, following features are read.

(i)The stress-strain curve shows also serration due to the intermittent breakage of the components and interfacial debonding.

(ii)In case (b) in Fig.3, as $\alpha_f < \alpha_m$, the matrix and fiber have tensile and compressive residual stresses along fiber axis, respectively. In the example of Fig.3, the average failure strain of the matrix was taken to be comparable with that of fiber under no residual stresses. The authors [3,4] have shown that the tensile residual stress in the matrix enhances the breakage of matrix and also hastens the matrix breakage-induced debonding, while the compressive one in the fiber retards the fracture of fiber and also suppresses the fiber breakage-induced debonding. Comparing the variation of broken matrix-elements N_M and debonded interface-elements N_I with increasing applied strain in case (b) with that in case (a), the former evidently shifts to lower strain range. As known from such a difference under the existence of the present residual stresses, the matrix breakage and matrix breakage–induced debonding occur in the early stage, resulting in loss of stress carrying capacity and therefore low strength of composite. On the other hand, in the composite without residual stresses (a), the matrix is broken nearly at the same strain of breakage of fiber and the premature debonding does not arise so much until the ultimate stress, resulting in high strength. As the deleterious effect of the present residual stresses on the strength of weakly bonded composites, the strength of the composite with residual stresses (b) was 930MPa, which was far lower than 1500MPa of the composite without residual stresses (a).

(iii) In the case of (b) in Fig.3, the matrix breakage and the interfacial debonding have occurred in the early stage.

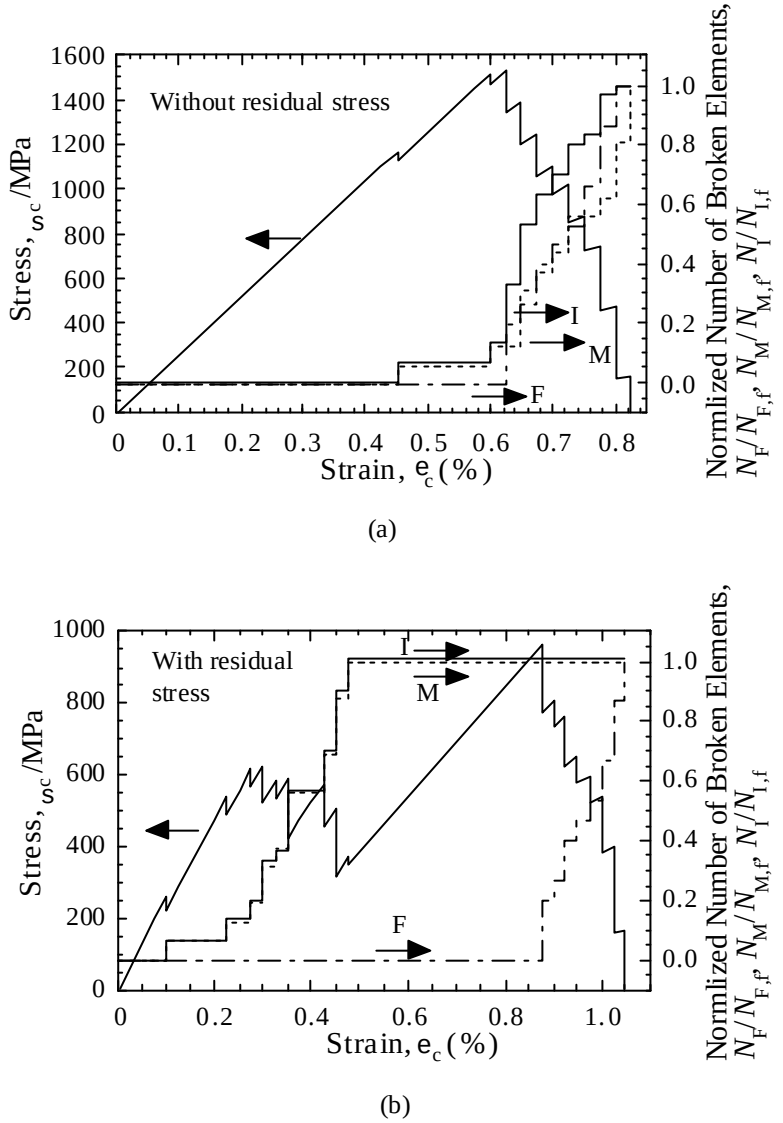

Figure 3 Comparison of the stress-strain curve, strength and accumulation process of damages between the composites (a) without and (b) with residual stresses.

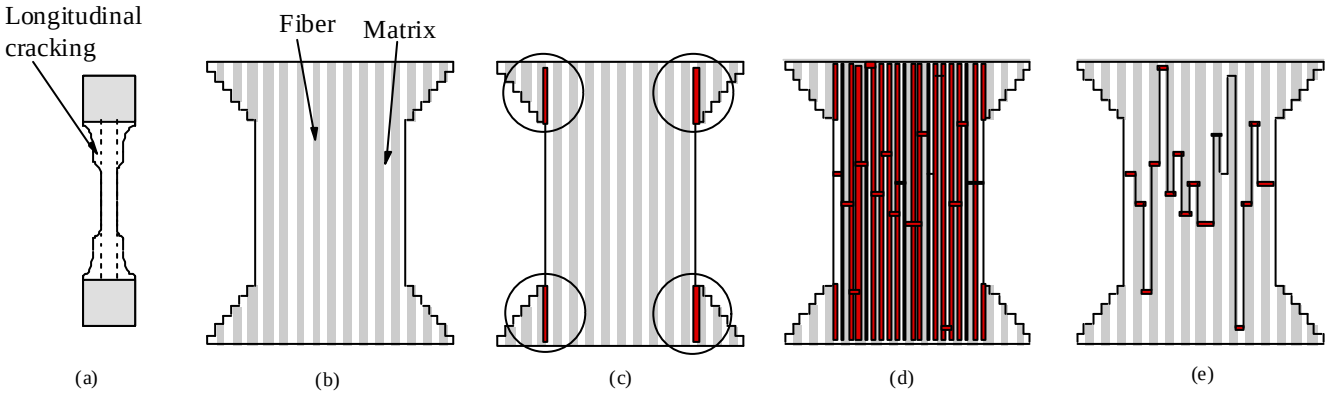

Figure 4 (a): Schematic drawing of the longitudinal cracking in the unnotched specimen. (b): Modeling for simulation. (c) to (e): Simulated fracture process accompanied with

longitudinal cracking and the fracture morphology

Once such a situation has occurred, the fibers are separated to each other and behave like a fiber bundle without matrix. Thus the strength of such composite is given by the strength of the fiber bundle. Further simulation using the low failure

strain-matrix composite without residual stresses showed the same feature.

(iv) It has been known that, in weakly bonded composites, longitudinal cracking occurs ahead of the notch. Furthermore, even in the unnotched samples, the longitudinal cracking between the parallel gage portion and the tapered one occurs (Fig.4(a)). Such a feature is also well realized in Fig.4 (b) to (e).

(v) It has been well known that the fiber is pulled-out in weakly bonded composites. The final fracture morphology of the composite, shown in Fig.4(e), describes such a feature also.

(vi) In notched samples, the longitudinal cracking occurs in the whole length between the grips at lower applied stress level than that in unnotched samples. Thus, the notch does not cause mode I type fracture but enhance longitudinal cracking. As a result, the strength of notched samples could be expressed by the net strength criterion.

CONCLUSIONS

The variation of the damage map, stress-strain curve, strength and fracture morphology of two-dimensional model composite with weak interface were simulated by combining the shear lag analysis with the Monte Carlo method. Following features of weakly bonded composites were described.

(1) Both of the breakage of components and interfacial debonding occur intermittently.

(2) As a result of (1), the stress-strain curve is serrated.

(3) When the fracture strain of matrix is low, the residual stresses (tensile and compressive stresses along fiber axis for matrix and fiber, respectively) enhance breakage of matrix and matrix breakage-induced debonding at low applied strain. As a result, the stress carrying capacity of the composite is reduced, resulting in low strength.

(4) The strength of weakly bonded composites whose matrix has low failure strain is practically given by the strength of the fiber bundle.

(5) Longitudinal cracking arises at the notch tip in notched specimens and also at the tapered corner in the unnotched specimens.

(6) The notched strength is given by the net stress criterion.

Acknowledgement

The authors wish to express their gratitude to The Ministry of Education, Science and Culture of Japan for the grant-in-aid for Scientific Research (No.11555175).

REFERENCES

1. Hedgepeth, J. M.. (1961). *Stress Concentrations in Filamentary Structures*. NASA TN D-882, Washington,.
2. Oh, K. P. (1979) *J. Comp. Mater.*, **13,** 311.
3. Ochiai, S., Okumura, I., Tanaka, M. and Inoue, T. (1998) *Comp. Interfaces*, **5**, 363.
4. Ochiai, S., Tanaka, M. and Hojo, M. (1998) *Comp. Interfaces*, **5**, 437.
5. Ochiai, S. Hojo, M. and T. Inoue. (1999) *Comp. Sci. Tech.*, **59**, 77.